

Received March 2, 2022, accepted March 25, 2022, date of publication April 1, 2022, date of current version April 7, 2022.

Digital Object Identifier 10.1109/ACCESS.2022.3164103

Human–Robot Collaboration in 3D via Force Myography Based Interactive Force Estimations Using Cross-Domain Generalization

UMME ZAKIA^{1,2} AND CARLO MENON^{1,2,3}, (Senior Member, IEEE)

¹Menrva Research Group, School of Mechatronic Systems Engineering, Simon Fraser University, Metro Vancouver, BC V5A 1S6, Canada

²School of Engineering Science, Simon Fraser University, Metro Vancouver, BC V5A 1S6, Canada

³Biomedical and Mobile Health Technology Laboratory, Department of Health Sciences and Technology, ETH Zürich, 8092 Zürich, Switzerland

Corresponding author: Carlo Menon (cmenon@sfu.ca)

This work was supported in part by the Natural Sciences and Engineering Research Council of Canada (NSERC), in part by the Canadian Institutes of Health Research (CIHR), and in part by the Canada Research Chair (CRC) Program.

ABSTRACT In this study, human robot collaboration (HRC) via force myography (FMG) bio-signal was investigated. Interactive hand force was estimated during moving a wooden rod in 3D with a Kuka robot. A baseline FMG-based deep convolutional neural network (FMG-DCNN) model could moderately estimate applied forces during the HRC task. Model performance can be improved with additional training data; however, collection of it was impractical and time-consuming. Available long-term multiple source data (32 feature spaces) during human robot interaction (HRI) with a linear robot collected over a long time period might be useful. Therefore, we explored a cross-domain generalization (CDG) technique that allowed pretraining a model to transfer knowledge between two unrelated source (2D-HRI) and target data (3D-HRC) for the first time. An FMG-based transfer learning with CDG (TL-CDG) model trained with these multiple source domains was examined in estimating applied forces from 16-channel FMG data during interactions with the Kuka robot. Two target scenarios were evaluated: *case i*) collaborative task of moving the wooden rod in 3D, and *case ii*) grasping interactions in 1D. In both cases, few calibration data finetuned the TL-CDG model and improved recognizing out-of-domain target data (*case i*: $R^2 \approx 60\text{--}63\%$, and *case ii*: $R^2 \approx 79\text{--}87\%$) compared to the baseline FMG-DCNN model. Hence, cross-domain generalization could be useful in platform-independent FMG-based HRI applications.

INDEX TERMS Force myography technique, long-term multiple source FMG data, human robot collaboration, cross-domain generalization, deep transfer learning.

I. INTRODUCTION

In common industrial collaborative tasks (such as object handover or transportation), a human worker mostly uses hand forces to interact with machines. Hence, in the literature, there are quite a few studies where interactive forces were estimated using bio-signals such as surface electromyography (sEMG) and force myography (FMG) techniques. As a contemporary technology like sEMG, FMG is a non-invasive, wearable technique that often utilizes force sensing resistors (FSRs) that detect changes in resistance when pressure is

applied [1]. An FMG band wrapped around an upper limb can be used in estimating grasping or isometric forces from muscle contractions [2], [3]. Therefore, FMG bio-signals can be useful in detecting certain human activities. Recently, FMG signals were used to recognize intentional or random hand movement during a human robot collaboration (HRC) task with an industrial YUMI manipulator robot [4]. In this study, human intention was identified by implementing a recurrent neural network (RNN). This RNN model was trained on intra-session data that allowed the robot to avoid collision in case of unintentional movements. In a present-day study, grasping forces from intra-session FMG data was investigated to classify the grasped object. This study focused in recognizing the

The associate editor coordinating the review of this manuscript and approving it for publication was Laura Celentano¹.

intended tool (object) to be used by the human worker during a shared HRC task [5]. In a follow up study, a generalized object classifier with inter-session grasping FMG data was found applicable to new users without prior training for an HRC task [6].

In recent sEMG-based human-robot interactions (HRI) studies, deep learning techniques such as convolutional neural networks (CNN) and long-term short memory (LSTM) were used for dynamic or static force estimations [7]–[9]. A few studies were conducted recently where FMG bio-signals were used for applied force estimations during physical human-robot interaction (pHRI) activities [10]–[12]. In [10], pHRI between several participants and a fixed linear robot was investigated using intra-session data. For each participant, a task-based machine learning (ML) model was trained with instantaneous applied force in a selected dynamic motion. Such an individual-specific, intra-session biased model predicted interactive forces ($94% > R^2 > 82%$) in real-time during the same session. Interestingly, pHRI with inter-session FMG data using domain adaptation and generalization in a planar workspace was recently investigated with improved force estimations [11], [12]. In these 2D-pHRI studies, a generalized model trained with long-term FMG distributions (collected over a period) predicted unseen target data during repetitive usage or during interactions with a new participant. The source and target domains in these studies had the same interactive 2D-pHRI environment and system setup with 32 FMG channels on the forearm and upper arm positions. However, conducting human robot collaborative tasks in 3D via FMG-based estimated forces in the control loop is not investigated so far.

In this study, FMG-based pHRI with a 7-dof (degree-of-freedom) Kuka robot (serial robot) was investigated by estimating grasping forces in dynamic motion for the first time. In the beginning of the study, a cylindrical gripper attached as the end-effector (EEF) was used for hand grasps to interact in certain directions of 1D, 2D and 3D workspace. In each case, an intra-session convolutional neural network (CNN) model could moderately estimate grasping forces in dynamic interactions. However, there are hardly any studies in literature conducting human robot collaborative task in 3D via FMG-based force estimations. Due to the dynamic nature of the task, tools involved and redundant degree-of-freedom of human arm in 3D, force estimation via this transient bio signal is challenging. Hence, in this study, we mainly focused on investigating an HRC task of moving a wooden rod in collaboration with the Kuka robot. A 16-channel FMG band was used to capture the muscle readings during the task. Intra-session trained model in this 3D-HRC task moderately estimated forces during evaluation and hence required further improvements.

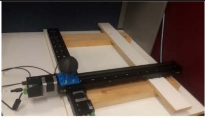
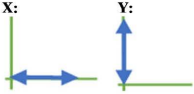
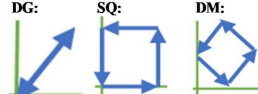

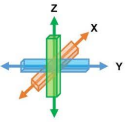
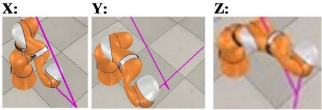
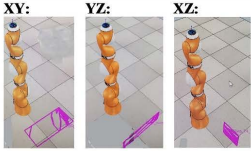

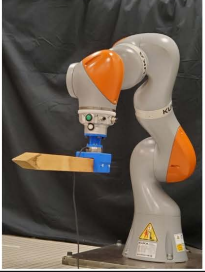
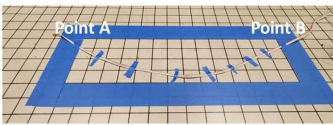
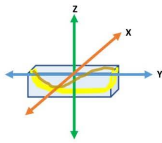
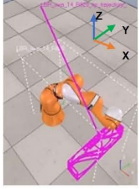



In practice, a generalized trained model with reduced dependencies on intra-session data is more desirable. Having more participations or collecting more inter-session data during the HRC task with the Kuka robot was not possible or practical due to time constraints. On the other hand,

a large volume of long-term data from other pHRI platform could be useful to reduce dependencies on intra-session data. Interestingly, cross-domain generalization (CDG) can be promising for unrelated source and target data that could allow a pretrained model to transfer knowledge between different platforms/systems. Furthermore, it generalizes beyond the source distributions [13], [14]. It could be useful and relevant to transfer knowledge learnt from interactions with a linear robot during interactions with a serial robot. The variations in individual-specific upper-limb muscle contractions, arm trajectories, body postures, no. of FMG channels and distinguished pHRI platform of different control system, signal capturing rate, software-hardware interfaces could contribute transferring knowledge between two distinct HRI applications. Cross-domain generalization is studied in image classifications, vision system, natural language processing, medical diagnosis, machine fault detects, etc. [15]–[19]. The CDG technique has been investigated in few studies conducted on human machine interfaces (HCI) and rehabilitations with surface electromyography (sEMG) or electroencephalography (EEG) bio signals [20]–[23]. However, it is not studied for bio signals based HRI tasks. Previously, FMG-based domain adaptation was examined with the same source and target platforms [12]. Therefore, the platform-independent FMG-based HRI via cross-domain generalization technique could be interesting and required further investigation [12].

Therefore, in this study, we conducted FMG-based HRC task to move the wooden rod using the supervised CDG technique. Multiple long-term source data from a 2D-pHRI platform was used in pretraining a transfer learner with CDG (TL-CDG) and was evaluated on a target 3D-HRC task for the first time. In an initial ‘training phase’, the long-term source domains (D_{s_i}) were collected when interactions occurred between several participants and a linear robot via 32-channel FMG bands. In this 2D-pHRI platform ($pHRI_{s_i}$), participant interacted by grasping a knob-like gripper/end-effector in the planar surface. In addition, a secondary pool of multiple source domains (D_{s_j}) via 16-channel FMG-based 3D-pHRI platform ($pHRI_{s_j}$) were also collected. In this 3D-pHRI, interactions occurred between a participant and a Kuka robot applying forces in 1D, 2D and 3D workspace while grasping a cylindrical gripper/end-effector. The secondary source data was used for comparative purposes only. Three separate TL-CDG models were pretrained with D_{s_i} data (TL-CDG-1), D_{s_j} data (TL-CDG-2), and aggregated D_{s_j} data (TL-CDG-3). These models were evaluated on two separate cross-platform ($pHRI_t$) target domains where a participant interacted with the Kuka robot such that: *case i*) HRC task of moving a wooden rod in 3D environment (target domain $D_{t_{3D}}$), as shown in Table 1, and *case ii*) HRI in 1D motions by grasping a cylindrical end-effector (target domain $D_{t_{1D-X,Y}}$), as shown in Table 1.

The primary goal was to investigate the 2D-based TL-CDG-1 transfer learner’s ability to predict out-of-domain HRC target data from unseen 3D pHRI platform. Hence, all

TABLE 1. HRI/HRC Experimental Setup.

pHRI	Experimental Setup	1D	2D	3D
HRI with a linear robot in 1D & 2D				NA
HRI with a Kuka robot in 1D, 2D & 3D	 	 For X# 0.4: 0.7 m(x), -0.3:0.2m(y), 0.4:0.42m(z) For Y# 0.6:0.6 m(x), -0.35:0.2m(y), 0.4:0.4m(z) For Z# 0.6:0.7 m(x), -0.3:0.2m(y), 0.25:0.7m(z)	 For XY # 0.45:0.65 m(x), -0.3:0.2m(y), 0.4:0.42m(z) For YZ # 0.6:0.62 m(x), -0.3:0.2m(y), 0.3:0.45m(z) For XZ # 0.45:0.65 m(x), -0.1:0.25m(y), 0.3:0.5m(z)	 X Dimension: 0.2: 0.6 m Y Dimension: -0.5:0.5 m Z Dimension: 0.2:0.7m
HRC with a Kuka robot in 3D (moving a wooden rod from point A to point B)			 X Dimension: 0.2: 0.6 m Y Dimension: -0.5:0.5 m Z Dimension: 0.2:0.7m	
32-channel forearm & upper arm FMG bands			16-channel forearm FMG band	 

pretrained TL-CDG models were evaluated in *case i* while the TL-CDG-1 model was evaluated in *case ii* only. Therefore, this study focused on:

1. investigating FMG-based HRC with a Kuka robot in 3D,
2. investigating HRC activities using reduced FMG channels and reduced intra-session training data dependency, and
3. investigating FMG-based deep transfer learning with cross domain generalization in HRC for the first time where $D_s \neq D_t$, $T_s \neq T_t$, and $pHRI_s \neq pHRI_t$.

The rest of the article is organized as follows. Section II describes the experimental setup, problem statement, methodology, and the protocol followed. Results and performance evaluations are discussed in Section III and IV respectively. Finally, we conclude this article in Section V.

II. MATERIALS AND METHODS

A. EXPERIMENTAL SETUP

1) pHRI SETUP FOR SOURCE DOMAINS D_s

In this FMG-based pHRI task, five human participants interacted with a fixed linear robot/biaxial stage, as shown in Table 1. The linear robot had two perpendicular linear stages

(X-LSQ450B, Zaber Technologies, Vancouver, BC, Canada)] in X and Y directions on a planar surface. A knob-like gripper was attached at the top. A 6-axis FT sensor (Mini45, ATI Industrial Automation, Apex, NC) was placed inside the knob that served as the true label generator. Compliant collaboration control allowed the gripper to slide along the workspace according to human applied force. The linear robot was placed securely on the planar surface of a table. Two FMG bands (32 feature space) using 32 FSRs (TPE 502C, Tangio Printed Electronics, Canada) were used to read forearm and upper arm muscle contractions as captured by data acquisition systems (NI DAQs 6259, 6341, National Instruments, Austin, TX, US). A Labview interface running on an HP Zbook laptop (Intel core i7, 16GB RAM) was used for data collection.

2) pHRI SETUP FOR SOURCE DOMAINS D_s

For this pHRI task, interactions between a participant and a Kuka robot (KUKA LBR IIWA 14 R820, KUKA Robotics, Augsburg, Germany) were observed in 1D, 2D and 3D space, as shown in Table 1. A 16-channel forearm FMG band was used to collect muscle contraction readings during interactions through NI DAQ 6341 (National Instruments,

Austin, TX, US). A custom-made cylindrical gripper was attached as the end-effector of the robot via a customized adapter. A 6-axis FT sensor (NI DAQ 6259, National Instruments, Austin, TX, US) was placed between the gripper and the adapter for true label generation. The orientation of the end-effector was always at $\{0, \pi, 0\}$, thus the gripper-handle pointed downwards for easy human grasps. The Kuka robot was securely mounted on a table and its surroundings were caged for safety measures. Compliant collaboration using torque control was implemented where the robot moved in space proportional to the applied human forces and directions. Matlab scripts were written (Matlab, Mathworks, Natick, MA, USA) using the Kuka Sunrise Toolbox to run externally on a desktop PC (Intel Core i7 processor and Nvidia GTX-1080 GPU) with V-REP robot simulator and to communicate with Kuka Sunrise Controller.

3) HRC SETUP FOR TARGET DOMAIN D_{t3D}

For HRC between the Kuka robot and a participant (P_6) in 3D space, a 45 cm rectangular wooden rod was attached to the end-effector of the robot, as shown in Table 1. The rod was firmly connected at one end [oriented at fixed angle $\{0, \pi, 0\}$] via a custom-made adapter while the other end was parallel with the horizontal X dimension in the 3D plane, free to grasp and apply force. The rod weighed approximately 5 lb including the adapter. A 6-axis FT sensor via NI DAQ 6259 was placed in between the adapter and the end-effector for true force readings. Interaction forces were applied at the tip of the cantilever rod and force readings of the FT sensor were adjusted by a factor δ (obtained experimentally). Matlab scripts were executed externally on a desktop PC (Intel Core i7 processor and Nvidia GTX-1080 GPU) and communicated with the Kuka Sunrise controller using Kuka Sunrise Toolbox. Compliant collaboration allowed participant to move the wooden rod from point A to point B in a half-circular 3D path where displacements and trajectories were governed by the applied forces and directions. A 16-channel forearm FMG band via NI DAQ 6341 was used to collect muscle contraction readings during the collaborative task.

B. PROBLEM STATEMENT

1) TRANSFER LEARNING FOR UNSEEN TARGET DOMAIN

In this study, transfer learning was investigated pretraining a cross-domain transfer learner using a primary set of five ($i=1, \dots, 5$) different long-term source domains such that $D_{si} \in \{X_{si}, Y_{si-X,Y,Z}\}$ ($X_{si}, Y_{si-X,Y,Z}$ were 32 feature spaces, and true force labels in 3D, respectively) collected from a 2D-pHRI (pHRI_{si}) platform. A secondary set of seven ($j=6, \dots, 12$) source domains $D_{sj} \in \{X_{sj}, Y_{sj-X,Y,Z}\}$ were also collected ($X_{sj}, Y_{sj-X,Y,Z}$: 16 feature spaces, and applied force labels, respectively) during interactions in a 3D-pHRI (pHRI_{sj}) platform. Each source domain D_s had a feature space of $X_s \in R_C^{N_s \times FMG}$ where N_s = no. of samples, $FMG_C = \{1, 2, \dots, C\}$ ($C = 32, 16$ for D_{si} and D_{sj}) and true force labels of F_{Xs}, F_{Ys}, F_{Zs} in X, Y, Z directions, respectively.

Applying feature engineering, a new input feature space X_{s*} was constructed such that:

$$\begin{aligned} X_{s*} &= [X_s, \overline{X_s}, \sigma(X_s)], \text{ for } D_{si}, \text{ and} \\ X_{s*} &= [X_s, \gamma(X_s), \overline{X_s}, \sigma(X_s)], \text{ for } D_{sj} \end{aligned} \quad (1)$$

where $\overline{X_s}$, $\gamma(X_s)$ and $\sigma(X_s)$ were the average, up sampled matrix, and variance of X_s , respectively. Therefore, all source domains became homogenous and balanced vectors ($34 \times N_s$ for each domain) suitable for deep CNN architecture. Target domain $D_t \in \{X_t, Y_{t-X,Y,Z}\}$ had feature space of $X_t \in R_C^{N_t \times FMG}$ where N_t = no. of samples, $FMG_C = \{1, 2, \dots, C\}$ ($C = 16$ FMG channels) and $Y_{t-X,Y,Z}$: true labels of applied forces in X, Y, Z directions (F_{Xt}, F_{Yt}, F_{Zt}). For evaluation, a new feature space was reconstructed as:

$$X_t^* = [X_t, \overline{X_t}, \gamma(X_t), \sigma(X_t)] \quad (2)$$

where $\overline{X_t}$, $\gamma(X_t)$ and $\sigma(X_t)$ were the average, up sampled matrix (up sampled to 32 channels) and variance of X_t , respectively. Hence, the target distributions had total feature spaces of ($34 \times N_t$) like the source domains for force mapping during evaluation. Adding few more features increased data variabilities in the feature spaces for a deep learning model to learn discriminative features better.

For the source task T_s , true labels of applied interaction forces ($Y_s: F_X, F_Y, F_Z$) were standardized according to:

$$Y_s^* = (Y_s - \overline{Y_s}) / \sigma(Y_s) \quad (3)$$

where $\overline{Y_s}$ and $\sigma(Y_s)$ were the average and variance of Y_s , respectively. Due to the planar workspace of D_{si} domains, F_Z was at minimal values (0.1N) as the force interactions were one-directional (1D) and two-directional (2D) only. A proposed deep transfer learning 'TL-CDG' model with a Φ of Ω parameter based on a unique CNN architecture (Section II.A.2) was used as feature extractor on $\{X_{s*}, Y_{s*}\}$ and the trained model with learnt weights were saved to evaluate target domain D_t .

At an instant in time, t , the pretrained TL-CDG model was used to evaluate target input FMG_C signals $\{X_t^*\}$ which was split into calibration data $\{X_C^* \subset X_t^*\}$ and validation data $\{X_D^* \subset X_t^*\}$. The calibration data (target training data) $\{X_C^*, Y_{C-X,Y,Z}\}$ was used to retrain the model for target adaptation. Afterwards, for target task $T_t \{Y'_{D-X,Y,Z}, \hat{f}(\cdot)\}$, a predictive function, $\hat{f}(\cdot)$ estimated interaction forces in the X, Y and Z directions on validation set (target test data) $\{X_D^*\}$ at the time t such that:

$$\hat{f}_x(\cdot) = F'_{XD} = \Phi, \quad (X_D^*, \Omega_1) \quad (4)$$

$$\hat{f}_y(\cdot) = F'_{YD} = \Phi, \quad (X_D^*, \Omega_2) \quad (5)$$

$$\hat{f}_z(\cdot) = F'_{ZD} = \Phi, \quad (X_D^*, \Omega_3) \quad (6)$$

The model attempted to find the best parameter space Ω , which was determined by computing the loss function using force label space $Y_{D-X,Y,Z}(F_{XD}, F_{YD}, F_{ZD})$ of target test data:

$$\Omega_1 = L(F'_{XD} - F_{XD}) = \arg \max_{\Omega_1} \sum_{q=1}^t (F'_{XD} - F_{XD})^2 \quad (7)$$

$$\Omega_2 = L(F'_{YD} - F_{YD}) = \arg \max_{\Omega_2} \sum_{q=1}^t (F'_{YD} - F_{YD})^2 \quad (8)$$

$$\Omega_3 = L(F'_{ZD} - F_{ZD}) = \arg \max_{\Omega_3} \sum_{q=1}^t (F'_{ZD} - F_{ZD})^2 \quad (9)$$

Root mean square error (RMSE) determined the average squared difference between the estimated and the real value. RMSE for a single observation was:

$$RMSE_x = \sum_{q=1}^W \frac{(F'_{XD} - F_{XD})^2}{W} \quad (10)$$

$$RMSE_y = \sum_{q=1}^W \frac{(F'_{YD} - F_{YD})^2}{W} \quad (11)$$

$$RMSE_z = \sum_{q=1}^W \frac{(F'_{ZD} - F_{ZD})^2}{W} \quad (12)$$

where W was the number of responses, F_{XD}, F_{YD}, F_{ZD} were the target force labels, and $F'_{XD}, F'_{YD}, F'_{ZD}$ were the predicted forces for a response q .

2) FMG-DCNN ARCHITECTURE

In this study, an FMG-based deep convolutional neural network (FMG-DCNN) architecture was proposed for pretraining a TL-CDG model. For FMG-based HRC in 3D, three separate models (Model X, Y and Z) were pretrained for predicting applied force in that direction using appropriate Equations (4)-(6). For pHRI in 1D (either in X, Y or Z direction), only one relevant model was pretrained. A homogenous matrix of 34 features was used as input for the model using Equation (1), as described in Section II.A.1. Input data was normalized (minmax scaling) and passed to the input image layer [image size 1×34 with ‘zerocenter’ normalization]. Few convolutional blocks were implemented sequentially where each block had a conv2d layer followed by a ReLu activation function and a batch normalization layer. For Model X and Y, two convolutional blocks (conv1 and conv2) were used while three blocks (conv1, conv2 and conv3) were used in Model Z. 32 and 16 filters in Model X, 64 and 32 filters in Model Y and 32, 16, 8 filters in Model Z were used in the consecutive convolution layers, respectively. Two fully connected layers (FC1 and FC2) with 20 and 10 connections followed the conv blocks in consecutive order. A final regression layer mapped the instant force from the incoming feature spaces. The 3×3 filters with a stride of 1 and a padding of 1 were used in each conv2d layer. For optimization, stochastic gradient descent (SGD) was implemented with a learning rate (LR) of 1E-05 for maximum 60 epochs during pretraining.

For transfer learning, each pretrained model was finetuned by reinitializing a fully connected layer before the final regression layer and retrained the model with target training data. The retrained model was evaluated on target test data with SGD optimizer, an LR of 1E-05 (1E-06 for Model Y) for a maximum of 60 epochs. MSE loss [Equation (10)-(12)]

was calculated to evaluate model performance in force estimations.

C. PERFORMANCE MATRICES

Statistical tools such as the coefficient of determination (R^2) and coefficient of correlation (Coeff), root mean square error (RMSE), and normalized RMSE (NRMSE) were used to evaluate performances of the TL-CDG models.

Coefficient of determination (R^2) was obtained by:

$$R^2 = \frac{\text{Explained variation}}{\text{Total variance}} \quad (13)$$

It was used to determine the correlations or dependencies of the dependent variable on the independent variable. R^2 values varied between 0 and 1 indicating how good the regression predictions could fit the test data.

Correlation coefficient (Coeff) was determined between the matrix of pairwise variables of the true and the predicted values incurred by the model such that:

$$R = \begin{pmatrix} 1 & \rho(A, B) \\ \rho(B, A) & 1 \end{pmatrix}, \quad (14)$$

where the Pearson correlation coefficient ρ was calculated between A and B variables. It had values between +1 and -1 indicating strong and positive relationship between the variables.

RMSE was calculated based on:

$$RMSE = \sqrt{\frac{1}{n} \sum_i (Y_{est} - Y_{true})^2} \quad (15)$$

where n was number of samples, Y_{true} was the true data and Y_{est} was the prediction made by the regression model at an instant i .

NRMSE was determined by the fraction of RMSE to the observed range of the measured data such that:

$$NRMSE = \frac{RMSE}{\text{mean}(Y)} \quad (16)$$

where Y was the measured data.

D. PROTOCOL

A total of 6 participants (P_1, \dots, P_6) volunteered in this study who had no prior knowledge about FMG technique. All participants were healthy, right-handed and their average age was 33 ± 8 years. Written consents were collected as approved by Office of Research Ethics, Simon Fraser University, British Columbia, Canada.

In the supervised cross-domain generalization protocol, training phase of long-term FMG data collection was followed by evaluation phase as shown in Fig. 2 and described below:

1) TRAINING PHASE

In this initial phase, multiple source domains were collected over a period of several months, and then several TL-CDG models were pretrained.

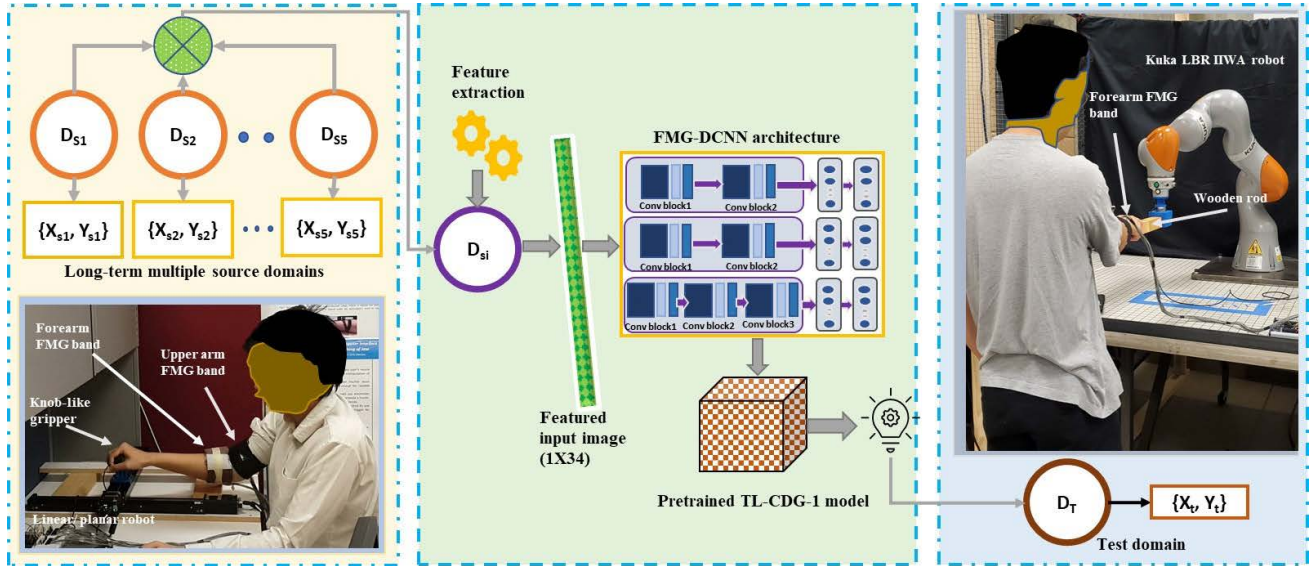


FIGURE 1. Cross-domain generalization via FMG-based SDG-TL-1 transfer learner in evaluating target HRC domain, $D_{t_{3D}}$ (moving a wooden rod with Kuka robot in 3D).

a: LONG-TERM MULTIPLE SOURCE DATA COLLECTION

i. PRIMARY SOURCE DOMAINS D_{s_i} $\{i=1, 2, \dots, 5\}$

Five participants (P_1, P_2, \dots, P_5) wearing two FMG bands on their forearm and upper arm on the dominant hand interacted with the fixed linear robot. Participants sat in front of the robot on a fixed-positioned chair [Fig. 2 (left)]. Each participant interacted with applied forces in five dynamic motions (source tasks, T_{s_i} $\{i = 1, 2, \dots, 5\}$) such as 1D ‘X’ (D_{s_1}), ‘Y’ (D_{s_2}), while ‘Diagonal’ (D_{s_3}), ‘Square’ (D_{s_4}) and ‘Diamond’ (D_{s_5}) in 2D plane in separate sessions, as shown in Table 1. These interactions included arm flexions, extensions and arm abduction, adductions in the planar space. For interactions in the 2D plane (‘Diagonal’, ‘Square’ and ‘Diamond’ motions), forces F_x and F_y acted in X and Y directions with F_z being at a constant value in the Z direction. In 1D interactions, only F_x or F_z acted in ‘X’ or ‘Y’ direction. A total of $50,000 \times 32$ FMG samples data were collected for the five source domains ($D_{s_1}, D_{s_2}, \dots, D_{s_5}$). Each participant performed 5 ‘repetitions’ (1 repetition: continuing interaction via applied force in a certain motion for approximately 1 min.) for each interactive task resulting in $2,000 \times 32$ samples. More information on the data collected in this setup are available in [10]. All distributions and dynamic motions were different in these primary sources ($D_{s_1} \neq D_{s_2} \neq D_{s_3} \neq D_{s_4} \neq D_{s_5}$, $T_{s_1} \neq T_{s_2} \neq T_{s_3} \neq T_{s_4} \neq T_{s_5}$).

ii. SECONDARY SOURCE DOMAINS D_{s_j} $\{j=6, 7, \dots, 12\}$

In these source data collections, participant (P_6) wearing a 16 channel FMG band on dominant (right) forearm stood steadily in one position in front of the Kuka robot, grasped the cylindrical gripper and applied forces in 1D [$D_{s_6} = ‘X’, D_{s_7} = ‘Y’$ and $D_{s_8} = ‘Z’$ dimensions], 2D [$D_{s_9} = ‘XY’, D_{s_{10}} = ‘YZ’$ and $D_{s_{11}} = ‘XZ’$ plane] and 3D plane

[$D_{s_{12}} ‘XYZ’$], as shown in Table 1. For compliant collaboration, trajectories of the Kuka robot were bounded by a 6-axis rectangular plane for an individual task [Table 1]. For each interaction in 1D, 2D, 3D, 5 repetitions of sample data were collected for training and evaluation purposes. Approximately, a total of $44,000 \times 16$ FMG samples data were collected from these source domains where all distributions and tasks were different ($D_{s_6} \neq D_{s_7} \neq D_{s_8} \neq D_{s_9} \neq D_{s_{10}} \neq D_{s_{11}} \neq D_{s_{12}}$, $T_{s_6} \neq T_{s_7} \neq T_{s_8} \neq T_{s_9} \neq T_{s_{10}} \neq T_{s_{11}} \neq T_{s_{12}}$).

b: PRETRAINING DEEP LEARNING MODELS

For cross domain generalization, three deep learning TL-CDG models were pretrained using the FMG-DCNN architecture such that: a) TL-CDG-1: using D_{s_i} domains only, b) TL-CDG -2: using D_{s_j} domains only, and c) TL-CDG -3: using D_{s_i} and D_{s_j} domains ($D_{s_i} \cup D_{s_j}$). All pretrained models had three separate models (Model X, Model Y, Model Z) for estimating interactive forces (F_x, F_y and F_z) in 3D motions, while only one model was used in 1D (Model X for 1D-X, and Model Y for 1D-Y). These models were saved as .mat files for evaluation phase.

E. EVALUATION PHASE

In this final phase, the two target domains: *case i*) HRC in 3D to move a wooden rod from point A to B ($D_{t_{3D}}$), and *case ii*) pHRI in simple motions in 1D ($D_{t_{1D=X,Y}}$) with cylindrical gripper were evaluated separately. In both cases, collected target data (5 repetitions: $\sim 6,400 \times 16$ FMG data) were divided into target training data (first 4 repetitions) and target test data (last repetition).

1) CASE I: TARGET DOMAIN, $D_{t_{3D}}$ (HRC IN 3D)

In each repetition, participant P_6 wearing 16 channels forearm FMG band stood in front of the Kuka robot, grasped the

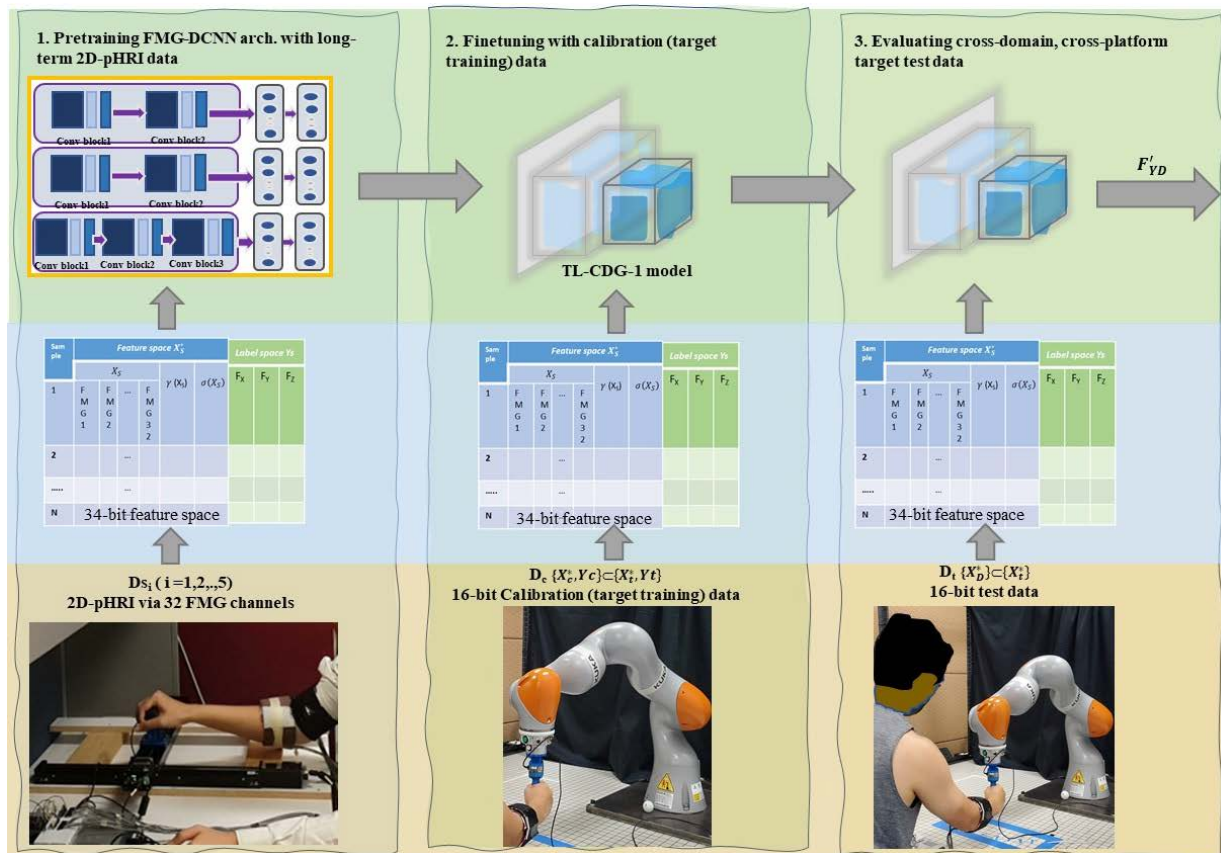


FIGURE 2. Transfer learning steps with TL-CDG-1 model for target domain, $D_{t_{1D-Y}}$: HRI in 1D-Y (traversing arm while grasping cylindrical EEF in right and left directions).

free end of the wooden rod and moved it collaboratively with the robot from point A to B and from point B to A repeatedly. The movements continued for a certain time (~ 2 min.) for one ‘repetition’ in a half-circular 3D trajectory path as the participant applied forces within his comfort zone. This was carried on 5 times collecting 5 repetitions of data, as shown in Fig. 1, and Table 1. All three pretrained TL-CDG models were finetuned with the target training data. The retrained target learner was then evaluated on target test data, thus resembling usual intra-session evaluation.

2) CASE II: TARGET DOMAIN, $D_{t_{1D-X,Y}}$ (pHRI IN 1D)

To observe how FMG-based generalization would impact pHRI with simple interactions, this special case was investigated with the TL-CDG-1 model only. This pretrained model was evaluated during pHRI between participant P_6 with Kuka robot in 1D-X and 1D-Y directions separately. Source domains D_{s_6} and D_{s_7} ($\sim 6,400 \times 16$ samples) were treated as $D_{t_{1D-X}}$ and $D_{t_{1D-Y}}$ where the first 4 repetitions were used for finetuning the TL-CDG-1 model, and the final repetition was used for model evaluation.

III. RESULTS

Pretraining the TL-CDG models and evaluations on target domain $D_{t_{3D}}$ (case i : HRC in 3D) and $D_{t_{1D-X,Y}}$ (case ii: pHRI in 1D) were carried out with MATLAB scripts using

deep learning toolbox, neural network toolbox, statistics and machine learning toolbox, signal processing toolbox running on a desktop PC (Intel Core i7 processor and Nvidia GTX-1080 GPU). Force estimations in target domains were evaluated using R^2 and *Coeff* while error in predictions was measured using *RMSE* and *NRMSE*, as reported of one minute evaluation for both case i and case ii in Table 2. Intra-session evaluation on the target domains (trained with 4 repetitions, tested on 5th repetition) were carried out using the baseline FMG-DCNN network to compare performances of the transfer learners in domain generalizations, as included in Table 2.

A. CASE I: HRC IN 3D (TARGET DOMAIN $D_{t_{3D}}$)

In this case, among the TL-CDG pretrained models, the TL-CDG-1 model was moderate in force estimation ($R^2 \approx 63\%$, *Coeff* $\approx 80\%$, *RMSE* $\approx 4.6N$, *NRMSE* ≈ 0.128) while TL-CDG-2 and TL-CDG-3 models had similar accuracies (SDG-TL-2: $R^2 \approx 60\%$, *Coeff* $\approx 77\%$ and TL-CDG-3: $R^2 \approx 62\%$, *Coeff* $\approx 79\%$) in force estimations and losses (SDG-TL-2: *RMSE* $\approx 4.8N$, *NRMSE* ≈ 0.13 and TL-CDG-3: *RMSE* $\approx 4.7N$, *NRMSE* ≈ 0.13). These reported results were obtained by averaging corresponding values of Model X, Y, Z of each TL-CDG model. An intra-session baseline FMG-DCNN model with same target training and target test data obtained lower performance than the transfer learners ($R^2 \approx 55\%$, *Coeff* $\approx 75\%$, *RMSE* $\approx 5.2N$, *NRMSE* ≈ 0.14 ,

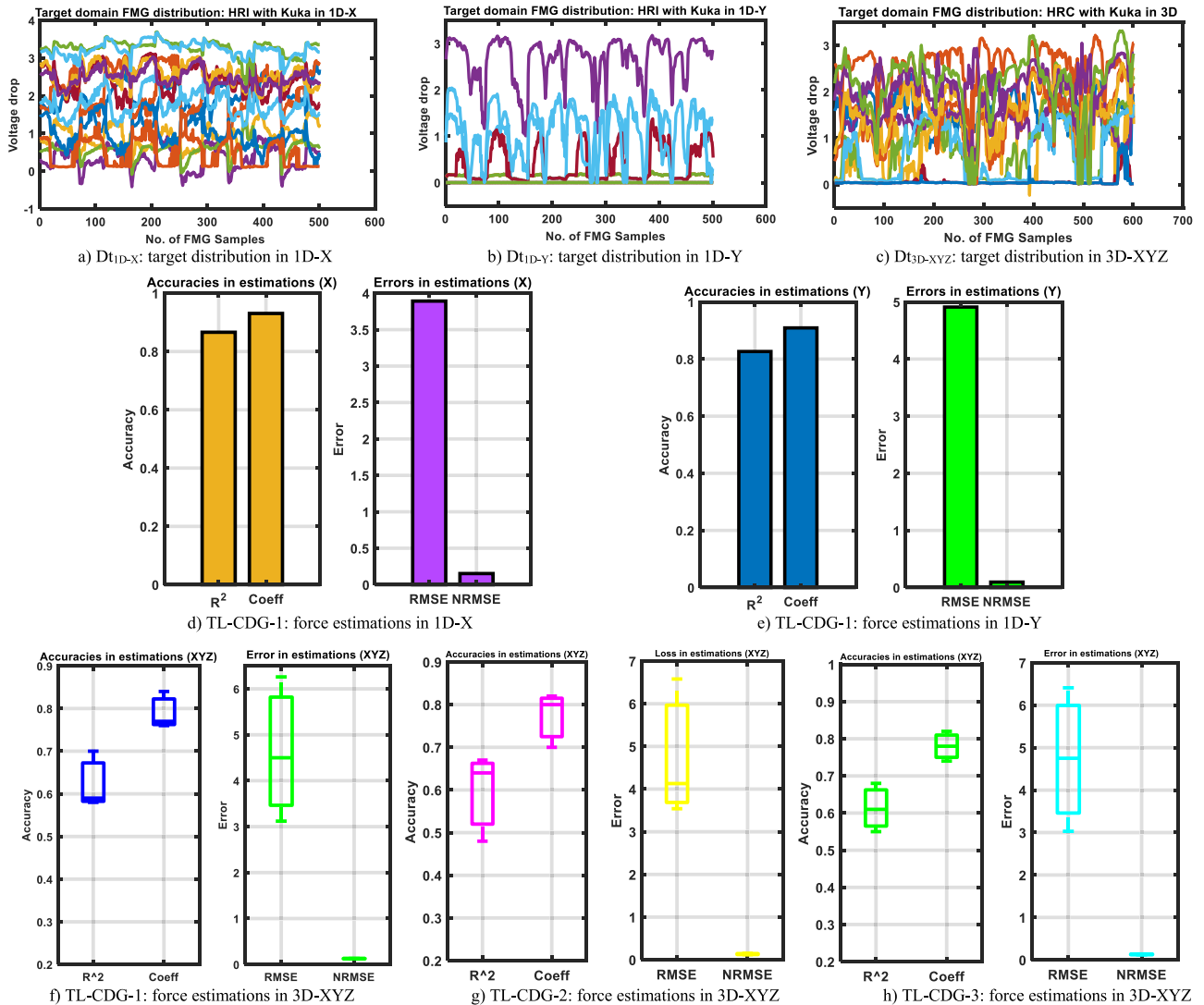


FIGURE 3. Few samples of target FMG distributions (a, b, c) and performances of the SDG-TL models (d,e: bar plot result for Model X and Y in 1D, and f, g, h: boxplot results for Model X, Y, Z in 3D).

where avg. values were obtained from X, Y, Z models). Hence, TL-CDG models clearly outperformed the baseline model with higher estimation accuracies and lower errors.

B. CASE II: pHRI IN 1D (TARGET DOMAIN D_{t1D})

In this case, TL-CDG-1 model was found effective in force estimations in X and Y dimensions once finetuned. Higher accuracies (X: $R^2 \approx 86\%$, $Coeff \approx 93\%$, and Y: $R^2 \approx 79\%$, $Coeff \approx 89\%$) and lower losses (X: $RMSE \approx 4.2N$, $NRMSE \approx 0.165$, and Y: $RMSE \approx 6.8N$, $NRMSE \approx 0.13$) were obtained by the TL-CDG-1 model than the intra-session baseline FMG-DCNN model (X: $R^2 \approx 77\%$, $Coeff \approx 88\%$, $RMSE \approx 3.6N$, $NRMSE \approx 0.14$, and Y: $R^2 \approx 66\%$, $Coeff \approx 81\%$, $RMSE \approx 5.8N$, $NRMSE \approx 0.11$). Although the baseline model estimated forces well, but the TL-CDG-1 model performed surprisingly well by transferring knowledge learnt from the 2D-pHRI long-term distributions.

IV. DISCUSSIONS

In this study, cross-domain generalization was observed during human robot interactions via the force myography technique. Transfer learning allowed the FMG-based TL-CDG model to predict unseen, unrelated and out-of-domain target data ($D_s \neq D_t$, $T_s \neq T_t$) on a different workspace ($pHRI_s \neq pHRI_t$). The source and target domains were distinctly dissimilar because of muscle readings captured by either 32 or 16 FMG channels positioned in different arm locations and separate HRI environments (different 1D/2D/3D workspaces, participant’s body posture during interactions, knob/cylinder/wooden rod as end-effectors). Since the gripper orientation and shapes were different, grasping forces and arm postures became distinctive. Also, participants applied interactive forces within their comfortable ranges (usually within 15N-40N) which was not constant. During the sessions, FMG bands were put on approximately same positions

TABLE 2. Performances of TL-CDG Models.

Target domain		Pretrained Model	R ²	Coeff	RMSE	NRMSE
Case i	<i>Dt_{3D}: HRC with Kuka in 3D (moving a wooden rod from point A to point B)</i>		X: 0.70 Y: 0.59 Z: 0.59	X:0.84 Y:0.76 Z:0.77	X:6.26 Y:4.50 Z:3.12	X:0.12 Y:0.13 Z:0.13
		1. TL-CDG-1	63%	79%	4.6N	0.13
		2. TL-CDG -2	60%	77%	4.75N	0.13
		3. TL-CDG-3	61%	78%	4.73N	0.15
		Baseline FMG-DCNN	56%	75%	5.11N	0.14
Case ii	<i>Dt_{1D-X}: pHRI with Kuka in 1D-X (interacting by grasping the cylindrical gripper)</i>	TL-CDG-1	86%	93%	3.58N	0.14
		Baseline FMG-DCNN	77%	88%	4.72N	0.18
	<i>Dt_{1D-Y}: pHRI with Kuka in 1D-Y (interacting by grasping the cylindrical gripper)</i>	TL-CDG-1	79%	89%	5.79N	0.11
		Baseline FMG-DCNN	66%	81%	7.28N	0.14

but were not exact; hence, sensors position shifts were possible in different sessions. Also, winding force to wrap the band around the limb was kept at the user’s comfort. Furthermore, collecting 5 repetitions of intra-session data were proven sufficient in capturing enough variabilities present during the interactions. Also, time required for one session was approximately 12-20 minutes and one repetition of interactions was less than 2min; these reduced muscle fatigue and ensured participant’s comfort.

Observations showed that intra-session baseline FMG-DCNN model with 34 feature space could obtain R² ≈56% in 3D force estimations while the TL-CDG models moderately improved accuracies in estimations [R² ↑ (2-8) %, Coeff ↑(2-7) %], with slight decrease in error [RMSE ↓≈ (0.2-0.5) N]. Among the pretrained models, the TL-CDG-1 model performed comparatively better in both simple and complex interactions in 1D and 3D. Clearly, the TL-CDG-1 model achieved significant improvements in estimation accuracies in 1D-HRI [R² in 1D-X (~10%↑), 1D-Y (~12%↑)], and in complex 3D-HRC [R² in 3D-XYZ (~8%↑)]. Fig. 3 shows target test FMG distributions during 1D and 3D interactions and the models’ performances plotted in bar plot and boxplot for ease of visualization. Since TL-CDG-2 and TL-CDG-3 models were already pretrained with source distributions of pHRI in 1D-X and 1D-Y, these were not investigated for case ii. HRI with Kuka in 1D-Z and 2D (XY, YZ, XZ) were not investigated due to time constraints. Furthermore, the constant Z dimension values in D_{s_i} restrained further exploration on this matter.

Source domains D_{s_i}{1,...,5} and target domains Dt_{3D}, Dt_{1D-X,Y} were different and the target data were totally unseen and out-of-distribution for the TL-CDG-1 model. Observations showed that this model could still predict OOD and unseen target data from a different HRI environment. Although, without fine-tuning with calibration data, the model would fail in estimating 3D-HRC task. Interestingly, the TL-CDG-1 model could predict simple 1D interactions fairly well. One reason could be that the source data used in pretraining this model had applied forces in arm flexion, extension, and arm abduction, adduction on the planar surface. Similar arm postures were also present in 1D-pHRI with Kuka robot. This phenomenon might help in the future design of an FMG-based HMI control system with safety mechanism. In a safety measures design, the TL-CDG pretrained model can be used for finetuning quickly with fewer target data for any participant. In a hazardous situation where human safety in pHRI might be breached, this can enable the participant to apply force on the robot and push away the robot from her/his proximity. Therefore, the proposed system can be implemented in human-robot safe collaborations in practical scenarios.

Initially, pHRI with Kuka robot by grasping the cylindrical gripper was investigated in this study using baseline FMGCNN architecture described in Section II.B.2. Separate intra-session model was trained with first 4 repetitions and evaluated on last 5th repetition for 1D (X, Y, Z directions), 2D (XY plane, YZ plane, XZ plane) and 3D (XYZ plane). The intra-session models were examined training with source distributions of 34 channel extended feature space based

TABLE 3. PHRI with Kuka: Intra-Session Evaluation with Baseline FMG-DCNN¹.

<i>pHRI with Kuka (Grasping a cylindrical gripper)</i>	<i>Feature engineering</i>	<i>Intra-session models</i>	<i>R²</i>	<i>Coeff</i>	<i>RMSE</i>	<i>NRMSE</i>
pHRI in 1D (X, Y, Z)	34 feature space	X: Model X Y: Model Y Z: Model Z	≥66%, ≤79%	≥81%, ≤89%	≥4.7N, ≤8.9N	≥0.14, ≤0.18
	16 feature space	X: Model X Y: Model Y Z: Model Z	≥78%, ≤81%	≥88%, ≤90%	≥4.0N, ≤8.0N	≥0.11, ≤0.16
pHRI in 2D (XY, YZ, XZ)	34 feature space	XY: Model X Model Y YZ: Model Y Model Z XZ: Model X Model Z	≥64%, ≤87%	≥80%, ≤93%	≥5.2N, ≤12.4N	≥0.12, ≤0.40
	16 feature space	XY: Model X Model Y YZ: Model Y Model Z XZ: Model X Model Z	≥64%, ≤87%	≥80%, ≤93%	≥5.6N, ≤12.2N	≥0.09, ≤0.16
pHRI with Kuka in 3D (XYZ)	34 feature space	XYZ: Model X Model Y Model Z	≥43%, ≤64%	≥65%, ≤80%	≥4.8N, ≤15N	≥0.13, ≤0.19
	16 feature space	XYZ: Model X Model Y Model Z	≥46%, ≤63%	≥68%, ≤80%	≥4.4N, ≤15.9N	≥0.12, ≤0.20
HRC with Kuka in 3D (XYZ) <i>(Moving a wooden rod in collaboration)</i>	34 feature space	XYZ: Model X Model Y Model Z	≥53%, ≤59%	≥73%, ≤77%	≥3.28N, ≤7.30N	≥0.13, ≤0.14
	16 feature space	XYZ: Model X Model Y Model Z	≥51%, ≤63%	≥85%, ≤90%	≥3.08N, ≤6.06N	≥0.12, ≤0.17

¹ Baseline FMG-DCNN model trained with 4 repetitions of target training data and evaluated on 5th repetition of target test data.

on Section II.B.1 and with raw 16 channel feature space to explore the effect of feature engineering. These results are summarized in Table 3. Although the baseline FMG-DCNN model could estimate similar with 16 or 34 feature space distributions, it was interesting to observe that the cross-domain TL-CDG-1 model with 34 feature space improved collaborative task performance of moving the wooden rod 3D, as well as improved grasping interactions in simple 1D-pHRI. Apparently, this TL-CDG-1 model could moderately improve grasping force estimation accuracies with lower errors during pHRI in 3D where cylindrical gripper was the end-effector (avg: $R^2 \leq 57\%$, $Coeff \leq 76\%$, $NRMSE \leq 0.153$, $RMSE \leq 8.1N$) with improvements. Collecting more inter-session training data from secondary sources could improve 3D-pHRI or 3D-HRC experiences for a shared task but requires more investigations in future.

For the target HRI with the Kuka robot, only one FMG band was used with a lesser number of channels to observe the impact of knowledge transfer from source domains that had more FMG channels. Interacting in 3D with only one forearm FMG band with a small amount of training data was a challenging task, which was reflected in the intra-session evaluation. However, the cross-domain generalization allowed the models to predict moderately well in 3D and better in 1D. Such generalization also helped reduce biases towards intra-session training data. An TL-CDG model with multiple source data can be more practical

because it would leverage periodic finetuning with less FMG data. Additionally, it reduces the need of collecting more labeled target training data and saves time. Therefore, cross-domain generalization via transfer learning could become an obvious choice for quick, practical FMG-based HRI implementation.

V. CONCLUSION

Transfer learning technique has been well-studied and applied successfully in image processing. This study showed that it could also be useful for FMG bio signal-based human-machine collaborative applications that required quick calibration with human data. Investigating deep transfer learning via cross domain generalization revealed the feasibility of conducting 16-channel HRC task. A transfer learning (TL-CDG-1) model pretrained with long-term FMG data from a 2D-pHRI obtained improved performances in force estimations for target pHRI in 1D ($86\% \geq R^2 \geq 79\%$) and moderately improved target HRC performance in 3D ($63\% \leq R^2$) with considerable increase in estimation accuracies for both cases [(5%-12%) \uparrow in R^2]. Also, finetuning the process helped addressing periodic calibration issues of instantaneous FMG signals using few target FMG data collected from forearm muscle belly. Therefore, this study addressed model cross-domain generalization beyond pHRI platform, solved calibration issues and bridged the gap in literature in FMG-based pHRI regression problem.

REFERENCES

- [1] Z. G. Xiao and C. Menon, "Towards the development of a wearable feedback system for monitoring the activities of the upper-extremities," *J. Neuroeng. Rehabil.*, vol. 11, no. 1, p. 2, 2014, doi: [10.1186/1743-0003-11-2](https://doi.org/10.1186/1743-0003-11-2).
- [2] M. Sakr, X. Jiang, and C. Menon, "Estimation of user-applied isometric force/torque using upper extremity force myography," *Frontiers Robot. AI*, vol. 6, p. 120, Nov. 2019, doi: [10.3389/frobt.2019.00120](https://doi.org/10.3389/frobt.2019.00120).
- [3] X. Jiang, L.-K. Merhi, and C. Menon, "Force exertion affects grasp classification using force myography," *IEEE Trans. Human-Machine Syst.*, vol. 48, no. 2, pp. 219–226, Apr. 2018, doi: [10.1109/THMS.2017.2693245](https://doi.org/10.1109/THMS.2017.2693245).
- [4] M. Anvaripour, M. Khoshnam, C. Menon, and M. Saif, "FMG- and RNN-based estimation of motor intention of upper-limb motion in human-robot collaboration," *Frontiers Robot. AI*, vol. 7, p. 183, Dec. 2020, doi: [10.3389/frobt.2020.573096](https://doi.org/10.3389/frobt.2020.573096).
- [5] N. D. Kahanowich and A. Sintov, "Robust classification of grasped objects in intuitive human-robot collaboration using a wearable force-myography device," *IEEE Robot. Autom. Lett.*, vol. 6, no. 2, pp. 1192–1199, Apr. 2021, doi: [10.1109/LRA.2021.3057794](https://doi.org/10.1109/LRA.2021.3057794).
- [6] E. Bamani, N. D. Kahanowich, I. Ben-David, and A. Sintov, "Robust multi-user in-hand object recognition in human-robot collaboration using a wearable force-myography device," *IEEE Robot. Autom. Lett.*, vol. 7, no. 1, pp. 104–111, Jan. 2022, doi: [10.1109/LRA.2021.3118087](https://doi.org/10.1109/LRA.2021.3118087).
- [7] H. Su, W. Qi, Z. Li, Z. Chen, G. Ferrigno, and E. De Momi, "Deep neural network approach in EMG-based force estimation for human-robot interaction," *IEEE Trans. Artif. Intell.*, vol. 2, no. 5, pp. 404–412, Oct. 2021.
- [8] Q. Zhang, L. Fang, Q. Zhang, and C. Xiong, "Simultaneous estimation of joint angle and interaction force towards sEMG-driven human-robot interaction during constrained tasks," *Neurocomputing*, vol. 484, pp. 38–45, May 2022, doi: [10.1016/j.neucom.2021.05.113](https://doi.org/10.1016/j.neucom.2021.05.113).
- [9] S. Kim, W. K. Chung, and K. Kim, "SEMG-based static force estimation for human-robot interaction using deep learning," in *Proc. 17th Int. Conf. Ubiquitous Robots (UR)*, Jun. 2020, pp. 81–86, doi: [10.1109/UR49135.2020.9144869](https://doi.org/10.1109/UR49135.2020.9144869).
- [10] U. Zakia and C. Menon, "Estimating exerted hand force via force myography to interact with a biaxial stage in real-time by learning human intentions: A preliminary investigation," *Sensors*, vol. 20, no. 7, p. 2104, Apr. 2020, doi: [10.3390/s20072104](https://doi.org/10.3390/s20072104).
- [11] U. Zakia and C. Menon, "Toward long-term FMG model-based estimation of applied hand force in dynamic motion during human-robot interactions," *IEEE Trans. Human-Machine Syst.*, vol. 51, no. 4, pp. 310–323, Aug. 2021, doi: [10.1109/THMS.2021.3087902](https://doi.org/10.1109/THMS.2021.3087902).
- [12] U. Zakia and C. Menon, "Force myography-based human robot interactions via deep domain adaptation and generalization," *Sensors*, vol. 22, no. 1, pp. 211–226, Jan. 2022, doi: [10.3390/s22010211](https://doi.org/10.3390/s22010211).
- [13] J. Wang, C. Lan, C. Liu, Y. Ouyang, T. Qin, W. Lu, Y. Chen, W. Zeng, and P. S. Yu, "Generalizing to unseen domains: A survey on domain generalization," 2021, *arXiv:2103.03097*.
- [14] E. Otović, M. Njirjak, D. Jozinović, G. Mauša, A. Michelini, and I. Štajduhar, "Intra-domain and cross-domain transfer learning for time series data—How transferable are the features?" *Knowl.-Based Syst.*, vol. 239, Mar. 2022, Art. no. 107976.
- [15] J. Zheng, C. Lu, C. Hao, D. Chen, and D. Guo, "Improving the generalization ability of deep neural networks for cross-domain visual recognition," *IEEE Trans. Cognit. Develop. Syst.*, vol. 13, no. 3, pp. 607–620, Sep. 2021, doi: [10.1109/TCDS.2020.2965166](https://doi.org/10.1109/TCDS.2020.2965166).
- [16] S. Paul, T. Dutta, and S. Biswas, "Universal cross-domain retrieval: Generalizing across classes and domains," in *Proc. IEEE/CVF Int. Conf. Comput. Vis. (ICCV)*, Oct. 2021, pp. 12056–12064.
- [17] J. Savelka, H. Westermann, and K. Benyekhlef, "Cross-domain generalization and knowledge transfer in transformers trained on legal data," Dec. 2021, *arXiv:2112.07870*.
- [18] Z. Ding and Y. Fu, "Deep domain generalization with structured low-rank constraint," *IEEE Trans. Image Process.*, vol. 27, no. 1, pp. 304–313, Jan. 2018, doi: [10.1109/TIP.2017.2758199](https://doi.org/10.1109/TIP.2017.2758199).
- [19] Y. Gu, Z. Ge, C. P. Bonnington, and J. Zhou, "Progressive transfer learning and adversarial domain adaptation for cross-domain skin disease classification," *IEEE J. Biomed. Health Informat.*, vol. 24, no. 5, pp. 1379–1393, May 2020, doi: [10.1109/JBHI.2019.2942429](https://doi.org/10.1109/JBHI.2019.2942429).
- [20] D.-K. Han and J.-H. Jeong, "Domain generalization for session-independent brain-computer interface," in *Proc. 9th Int. Winter Conf. Brain-Comput. Interface (BCI)*, Feb. 2021, pp. 1–5, doi: [10.1109/BCI51272.2021.9385322](https://doi.org/10.1109/BCI51272.2021.9385322).
- [21] J. Qi, G. Jiang, G. Li, Y. Sun, and B. Tao, "Intelligent human-computer interaction based on surface EMG gesture recognition," *IEEE Access*, vol. 7, pp. 61378–61387, 2019, doi: [10.1109/ACCESS.2019.2914728](https://doi.org/10.1109/ACCESS.2019.2914728).
- [22] Y. Guo, X. Gu, and G.-Z. Yang, "MCDGD: Multi-source unsupervised domain adaptation for abnormal human gait detection," *IEEE J. Biomed. Health Informat.*, vol. 25, no. 10, pp. 4017–4028, Oct. 2021, doi: [10.1109/JBHI.2021.3080502](https://doi.org/10.1109/JBHI.2021.3080502).
- [23] Z. He, Y. Zhong, and J. Pan, "An adversarial discriminative temporal convolutional network for EEG-based cross-domain emotion recognition," *Comput. Biol. Med.*, vol. 141, Feb. 2022, Art. no. 105048, doi: [10.1016/j.compbiomed.2021.105048](https://doi.org/10.1016/j.compbiomed.2021.105048).



UMME ZAKIA received the B.Sc. degree in electronics & computer science from Jahangirnagar University, in 2001, and the M.Sc. degree in computer science & engineering from North South University, Bangladesh, in 2007. She is currently pursuing the Ph.D. degree in engineering science with Simon Fraser University, BC, Canada. She is also working as a Research Assistant with the Menrva Research Group. She has published several articles in peer-reviewed journals and conferences. Her research interests include machine learning, robotics, HRI, communication networks, and VLSI.



CARLO MENON (Senior Member, IEEE) received the Laurea and Ph.D. degrees from the University of Padua, Italy, in 2001 and 2005, respectively. He was a Visiting Graduate Student with Carnegie Mellon University, USA, in 2004. He took a research fellow position with the European Space Agency, The Netherlands, in 2005 and 2006. He subsequently became a Professor with Simon Fraser University, Canada, where he founded the Menrva Research Group, held the Tier I Canada Research Chair and received a number of scholar awards, including both the Canadian Institutes of Health Research (CIHR) and the Michael Smith Foundation for health research awards. He joined ETH Zürich, in 2021, where he currently leads the Biomedical and Mobile Health Technology Laboratory. He has published over 300 articles in journals and conferences.

...